THE ASTROPHYSICAL JOURNAL, 290:L15–L20, 1985 March 1

MOLECULAR CLOUDS IN THE CARINA ARM

R. S. COHEN,[1] D. A. GRABELSKY,[1] J. MAY,[2] L. BRONFMAN,[1,2] H. ALVAREZ,[2] AND P. THADDEUS[1,3]
Received 1984 October 1; accepted 1984 November 21

ABSTRACT

From a new survey of the 2.6 mm line of CO in the southern Milky Way, we have been able to identify 37 molecular clouds along the Carina arm from $l = 282°$ to 336° with masses generally greater than $10^5\ M_\odot$. The clouds lie approximately every 700 pc along a spiral segment that is nearly 25 kpc long and has a pitch of about 10°. The total mass of these clouds is $40 \times 10^6\ M_\odot$, or roughly $1 \times 10^6\ M_\odot$ each on average. The abrupt tangent point in molecular clouds at $l = 280°$ and the characteristic loop structure in the l-v diagram are unmistakable evidence of a CO spiral arm in Carina. This arm apparently connects with the northern hemisphere Sagittarius arm to form a single 10° spiral which extends more than two-thirds of the way around the Galaxy.

Subject headings: galaxies: Milky Way — interstellar: molecules

The Carina arm, long since identified as a major feature of the Galaxy, is prominent in all tracers of spiral structure. Optically, it stands out from 2 kpc from the Sun to its tangent point at $l = 282°$ at 4 kpc (Graham 1970); some Carina arm stars and optical H II regions have been seen as far away as 10 kpc (Graham 1970; Georgelin and Georgelin 1976). In the radio thermal continuum the large step at $l = 282°$ (Mathewson, Healy, and Rome 1962) indicates a tangent point. On the 21 cm longitude-velocity diagram, a lane of emission traces the arm from just beyond the tangent point to a distance of more than 20 kpc (Kerr 1983).

Giant molecular clouds are even more confined to spiral arms than H I clouds, and their association with other Population I objects, such as young stars and H II regions, ties the radio arms to the local optical arms. Using data from the Columbia 1.2 m millimeter-wave telescope in New York, we previously located the largest molecular clouds in the northern hemisphere (Cohen *et al.* 1980; Dame *et al.* 1984) and found that they outline both the Perseus arm, at 12 kpc from the galactic center, and the Sagittarius arm, at 6–9 kpc. The only previous survey of molecular clouds near the Carina arm tangent (the 1.3 mm CO map of Israel *et al.* 1984) did not detect the arm because the sampling was sparse (> 1°), the observations were confined to the galactic plane, and the noise was high (0.4–0.8 K).

In 1983 January we installed a copy of the New York telescope at Cerro Tololo (Cohen 1982) and began a survey of the galactic distribution of molecular clouds in the southern Milky Way using the 2.6 mm CO line. That survey, now complete over most of the fourth galactic quadrant, contains the Carina arm discussed in this *Letter*.

A longitude-velocity diagram of our data (Fig. 1) shows the unmistakable signature of a spiral arm. The emission traces a characteristic loop which follows the rotation curve ridge at negative velocities, comes to a tangent point at $l = 280°$, and continues as a positive velocity lane to $l = 329°$. A wide gap in velocity, which is almost free of emission except for low-velocity local material, separates the near and far parts of the arm. This gap corresponds to an interarm region, free of massive molecular clouds, that lies inward of the Carina arm. The absence of emission to the right of the positive velocity part of the arm indicates an absence of clouds outward of the arm. The intense emission from the tangent point begins abruptly at the outer edge of the arm at $l = 280°$ and, as the line of sight moves through the center of the arm, broadens rapidly with increasing l, covering 40 km s^{-1} by 282°. In contrast, the rest of the low-velocity emission, which has much narrower lines and wider latitude extent (Fig. 2*b*), is primarily local. In particular, the narrow lane that extends from the tangent point to the bottom of Figure 1 is probably a single nearby object.

Figure 2 shows the Carina arm clouds, divided into three velocity ranges, on the plane of the sky. The low-velocity map (Fig. 2*b*) shows both the tangent region near $l = 282°$ and the wide local cloud at 270°–275°. The rest of the Carina arm extends to higher l as a thin layer of emission, on the near side of the tangent point at negative velocities (Fig. 2*a*) and on the far side at positive velocities (Figs. 2*c* and 2*d*). As expected, the layer on the near side is thicker in latitude than the collection of clouds at the tangent point, while the layer on the far side becomes progressively thinner as it proceeds from the tangent point toward $l = 329°$, where the arm is over 20 kpc away. In the most distant part of the arm even the smallest detectable CO features correspond to quite massive clouds; for example, the cloud at $l = 328°.5$ has a mass of about 330,000 $M_\odot$.

To locate the major Carina clouds in the Galaxy, we first prepared a catalog (Table 1) by dividing the distant emission into 38 major cloud complexes. We picked out objects similar to the largest complexes seen in the northern sky (Dame *et al.* 1984), of order 100 pc in diameter and 10^5–$10^6\ M_\odot$. In approximately half the cases, clouds were isolated and the division was unambiguous. In other cases, particularly the confused area near the Carina tangent, the catalog remains

[1] Columbia University.
[2] Universidad de Chile.
[3] Goddard Institute for Space Studies.

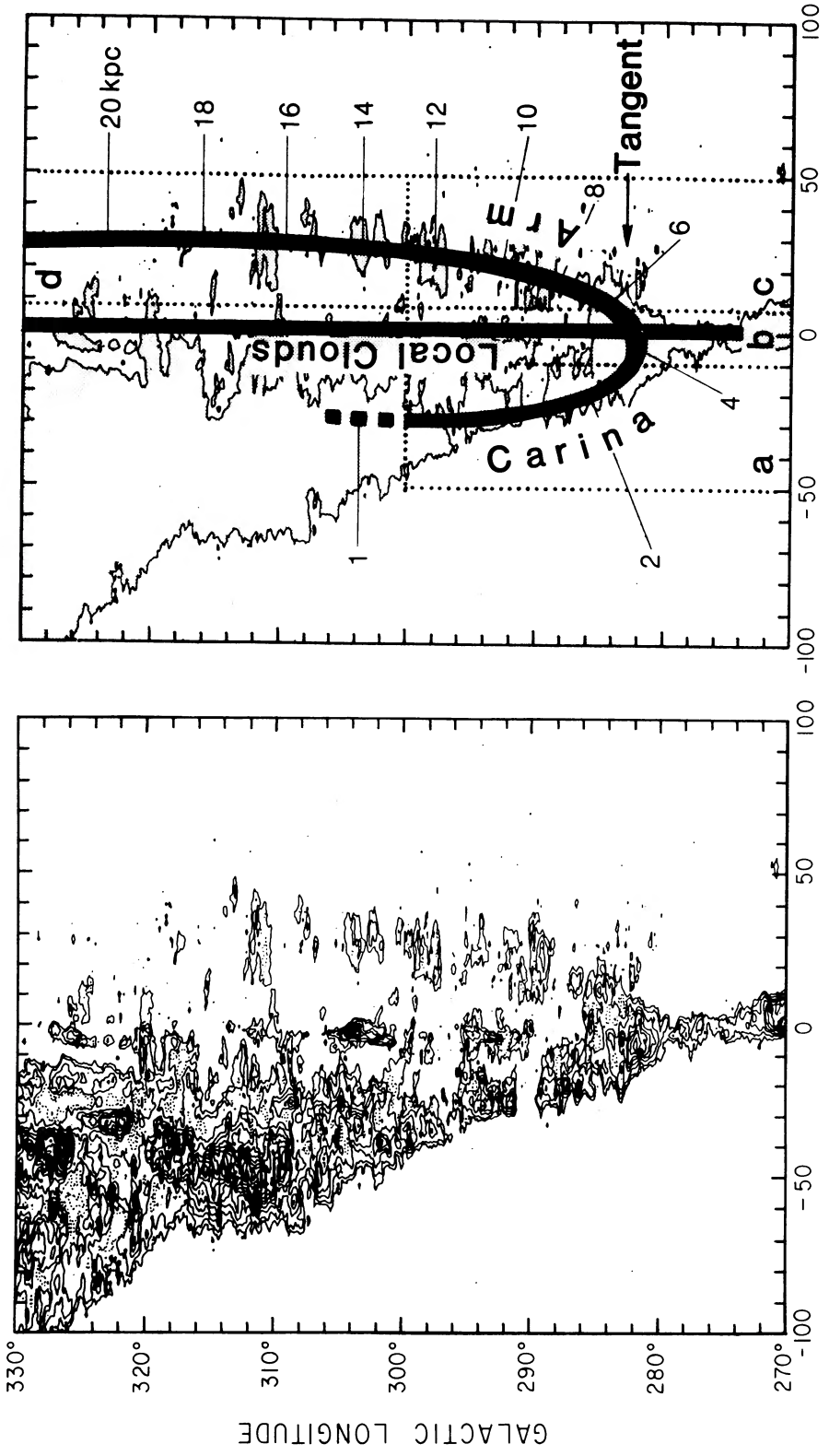

FIG. 1.—(*left*) Longitude-velocity diagram of CO emission integrated over latitude in all regions where observations were made on a 0°125 grid, i.e., approximately every beamwidth. (The coverage is shown in Fig. 2.) The contours are at 0.35, 0.7, 1.4, 2.1, 2.8,... K degree. The velocity resolution is 1.3 km s^{-1}, and the velocity coverage extends beyond the edges of the figure. The large blank areas, both beyond the far Carina arm and in the forbidden region at the lower left, demonstrate that this diagram is essentially free of noise. Every feature represents CO emission, and, in the farthest part of the arm, every feature represents a massive cloud. The first contour is at the 4 σ level. (*right*) Key. Approximate heliocentric distances are marked off along the Carina arm. The dark lines are schematic and are not derived from a model. The regions enclosed in dotted lines and labeled *a*, *b*, *c*, and *d* correspond to the four similarly labeled parts of Fig. 2. The crowded region in the upper left of the diagram will be discussed elsewhere.

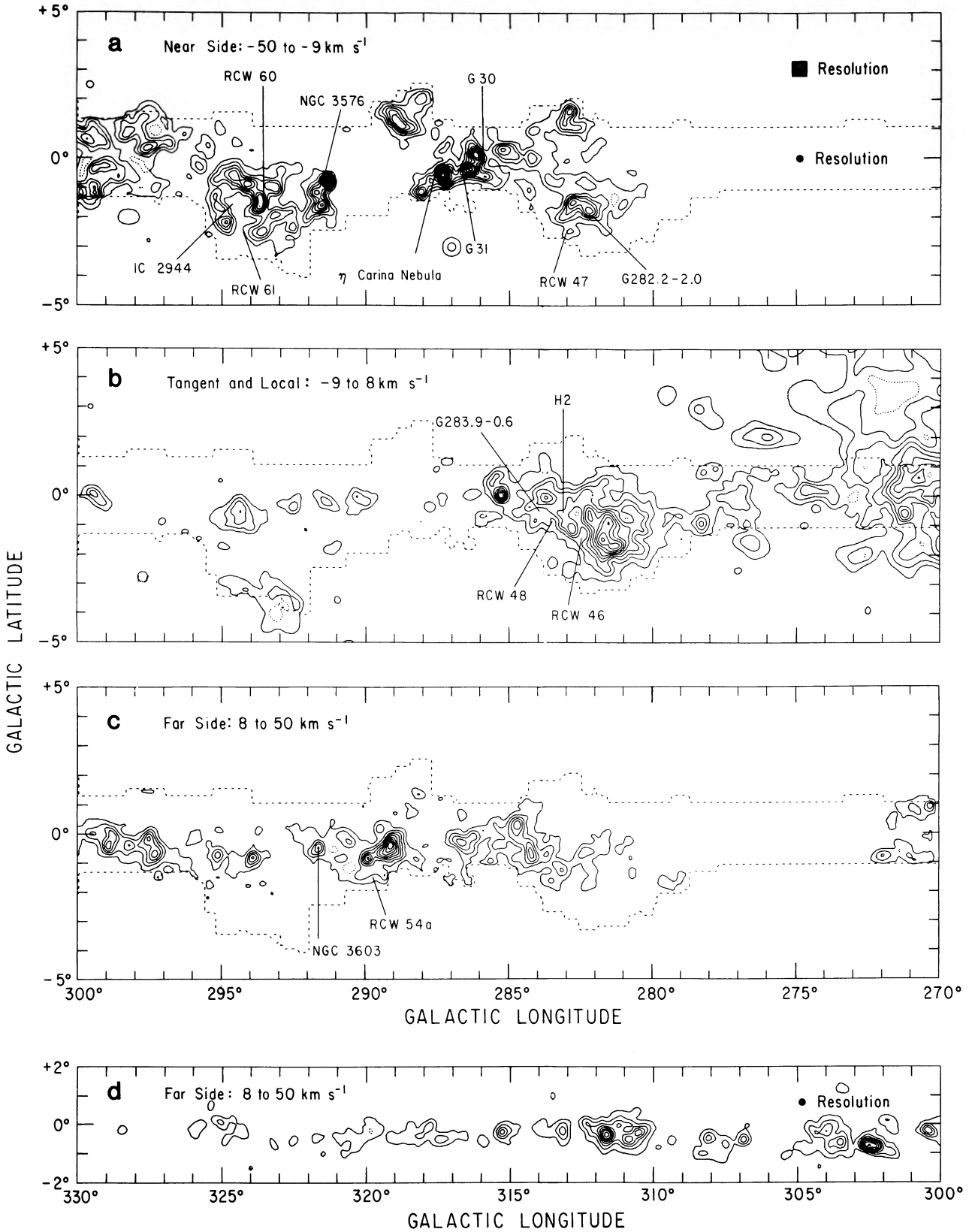

FIG. 2.—Maps of CO emission integrated over the indicated velocity ranges. Part (*a*) contains the near side of the Carina arm; part (*b*), the tangent region; and parts (*c*) and (*d*), the far side. The contour interval is 3 K km s^{-1}. From $l = 270°$ to 300°, observations were spaced every beamwidth. At high latitudes (outside the dotted lines) spectra were taken rapidly, smoothed to 0°.5 resolution, and then clipped (all channels below 0.5 K set to zero) to improve the signal-to-noise ratio. At low latitudes the spectra were smoothed to 0°.25 resolution but not clipped. From $l = 300°$–330°, at $|b| \leq 0°.75$ observations were spaced every beamwidth (0°.125) and smoothed to 0°.25, and at $1° < |b| \leq 2°$ observations were spaced every two beamwidths but not smoothed further. The resulting maps are essentially noise free. The figure indicates the optical H II regions used to determine distances to associated molecular clouds. The unusually low optical extinction in Carina is explained by a gap in the local clouds in the direction of the arm; the only large local cloud, which extends off the right-hand edge of part (*b*), ends fortuitously at $l = 275°$.

TABLE 1

LARGEST CARINA ARM MOLECULAR CLOUDS

l, b (°)	v_{LSR} (km s^{-1})	d[a] (kpc)	Mass (10^5 $M_\odot$)	Identification[b]
271.5, −0.5[c]	53	8.0	2	...
282.0, −1.5.....	−5	3.2	18	G282.2−2.0; RCW 46
282.3, −0.5.....	15	6.4	5	...
283.8, +0.0.....	−5	3.9	4	G283.9−0.6
284.5, +0.0.....	12	6.6	14	...
285.3, +0.0.....	0	5.3	3	H18
286.8, −0.3.....	14	7.5	6	H8
287.5, −0.5.....	−19	2.7	5	η Car nebula; G30, 31
288.8, +1.5.....	−22	3.2	3	...
289.3, −0.5.....	22	7.9	27	RCW 54a
290.3, +0.0.....	−1	6.8	2	...
291.4, −0.8.....	−25	3.3	2	NGC 3576
291.5, −0.4.....	15	7.2	3	NGC 3603
291.5, −0.8.....	29	10.3	9	H58
294.0, −0.8.....	32	11.3	9	...
294.0, −1.5.....	−25	2.4	4	IC 2944; RCW 60, 61
294.5, −0.5.....	−3	8.0	9	...
295.1, −0.8.....	26	11.0	3	...
297.3, −0.5.....	22	11.2	23	...
298.0, +0.0.....	−35	4.7	19	...
299.0, −0.5.....	25	12.0	23	G298.2−0.3
299.5, +0.0.....	−6	9.4	3	...
300.3, −0.2.....	31	12.9	5	...
300.6, −0.2.....	10	11.1	3	...
301.8, +0.0.....	24	12.7	3	...
302.3, −0.7.....	32	13.6	21	...
303.9, −0.4.....	29	13.7	33	...
306.9, −0.5.....	25	14.2	4	...
308.0, −0.7.....	32	15.1	15	...
311.3, −0.3.....	27	15.5	78	...
313.2, −0.3.....	42	17.6	13	...
314.0, −0.1.....	28	16.4	3	...
315.3, −0.3.....	14	15.4	8	...
318.0, −0.3.....	30	17.6	23	...
320.5, −0.5.....	26	17.8	9	...
325.3, −0.1.....	28	19.3	14	...
328.5, −0.1.....	30	20.4	4	...
335.5, −0.5.....	27	22.0	0.4	...

[a] Heliocentric distance.

[b] Partial list of associated optical and radio objects: RCW = Rodgers *et al.* 1960; G = Gum 1955; H = Hoffleit 1953; the first two sources denoted by galactic coordinates are from Bigay *et al.* 1972, the last from Wilson *et al.* 1970.

[c] Probably beyond the Carina arm (see text).

subject to minor revisions, but the uncertainties have little effect on the location or continuity of the arm.

Many of the molecular clouds in the catalog are associated with well-known objects that outline the optical Carina arm. For example, the large cloud on the plane between $l = 285°$ and 288° in Figure 2*a* is associated with three optical H II regions: G30, G31, and the Eta Carinae nebula. These H II regions fall close to CO emission peaks, and, measured either from radio recombination lines or from associated stars, their radial velocities fall within a few km s^{-1} of the CO velocities. Their distances are close to 2.7 kpc, which we may assume is the distance to the cloud. The cloud's diameter, 100 pc, and its mass, 5×10^5 $M_\odot$, are typical of the large complexes found in the first quadrant.

We assigned a distance to each cataloged cloud, either kinematically or, when possible, by association with an optical object with a known distance. Beyond the solar circle (at positive velocities), kinematic distances, used in all but two cases, are free of ambiguity and not very sensitive to the rotation curve. Inside the solar circle (negative velocities), where kinematic distances suffer from either inaccuracy near the terminal velocity ridge or a twofold ambiguity, optical objects with known distances locate three of the five clouds: the Eta Carinae nebula at 2.7 kpc, NGC 3576 at 3.3 kpc, and IC 2944 at 2.4 kpc. Near the tangent point (zero velocity), where kinematic distances are inaccurate, approximately half the clouds have optical distances.

In a face-on view of the Galaxy (Fig. 3) we plotted each cataloged cloud. From $l = 270°$ to 300° all the clouds fit into the Carina arm. The most likely exceptions are the cloud shown as a dashed circle, whose distance is very uncertain, and the cloud at $l = 271°$, $v = 52$ km s^{-1}, almost certainly well beyond the Carina arm. For the region from $l = 300°$ to 348°, the analysis is not yet complete except at positive velocities where all the largest clouds fit once again into the Carina arm, here about 2 kpc beyond the solar circle. The appearance of a cloud of 40,000 $M_\odot$ at 22 kpc from the Sun indicates that the catalog is complete to very great distances. A cloud appears on average every 700 pc along the arm.

Joining arms in the fourth quadrant to those in the first is a problem with a long history. According to the Georgelin and Georgelin (1976) model, which is based mainly on optical data, the Sagittarius and Carina arms form a single high-pitch spiral. As evidence against the Carina-Sagittarius connection, Kerr and Kerr (1970) cite a gap from $l = 292°$ to 304° in the 11 cm continuum and H109α fluxes. They propose a lower pitch model in which the first quadrant Sagittarius arm joins an inner fourth quadrant arm and the Perseus arm extends through the Sun to join the Carina arm beyond the solar circle.

The molecular cloud data distinctly favor the high-pitch model. No evidence exists for a large gap in the CO clouds: Figure 2*a* shows the near Carina arm continuing without interruption to the end of the analyzed region at $l = 300°$. As Figure 3 shows, any gap in the unanalyzed region at $l > 300°$ would represent a small path length that would be entirely consistent with other irregularities of the arm and fluctuations in the number of large clouds. On the other hand, any connection from Carina to an outer arm in the northern hemisphere would have a gap of at least several kiloparsecs. The density of molecular material is similar in the Carina and Sagittarius arms. The total mass in the Carina arm in molecular clouds greater than 10^5 $M_\odot$, 40×10^6 $M_\odot$, is spread over a 23 kpc path, yielding an average mass per length of 1.7×10^6 $M_\odot$ kpc^{-1}. The corresponding numbers in Sagittarius are 28×10^6 $M_\odot$ over 16 kpc, to yield 1.8×10^6 $M_\odot$ kpc^{-1}, or about the same as Carina. In contrast, in the Perseus arm we find 7×10^6 $M_\odot$ over 8 kpc, for 0.9×10^6 $M_\odot$ kpc^{-1}. When the clouds are plotted in galactocentric angle versus logarithm of galactic radius (Fig. 3, *right*), all the Sagittarius and Carina clouds evidently fall close to a single 10° logarithmic spiral; the pitch is fairly insensitive to the rotation curve. The most

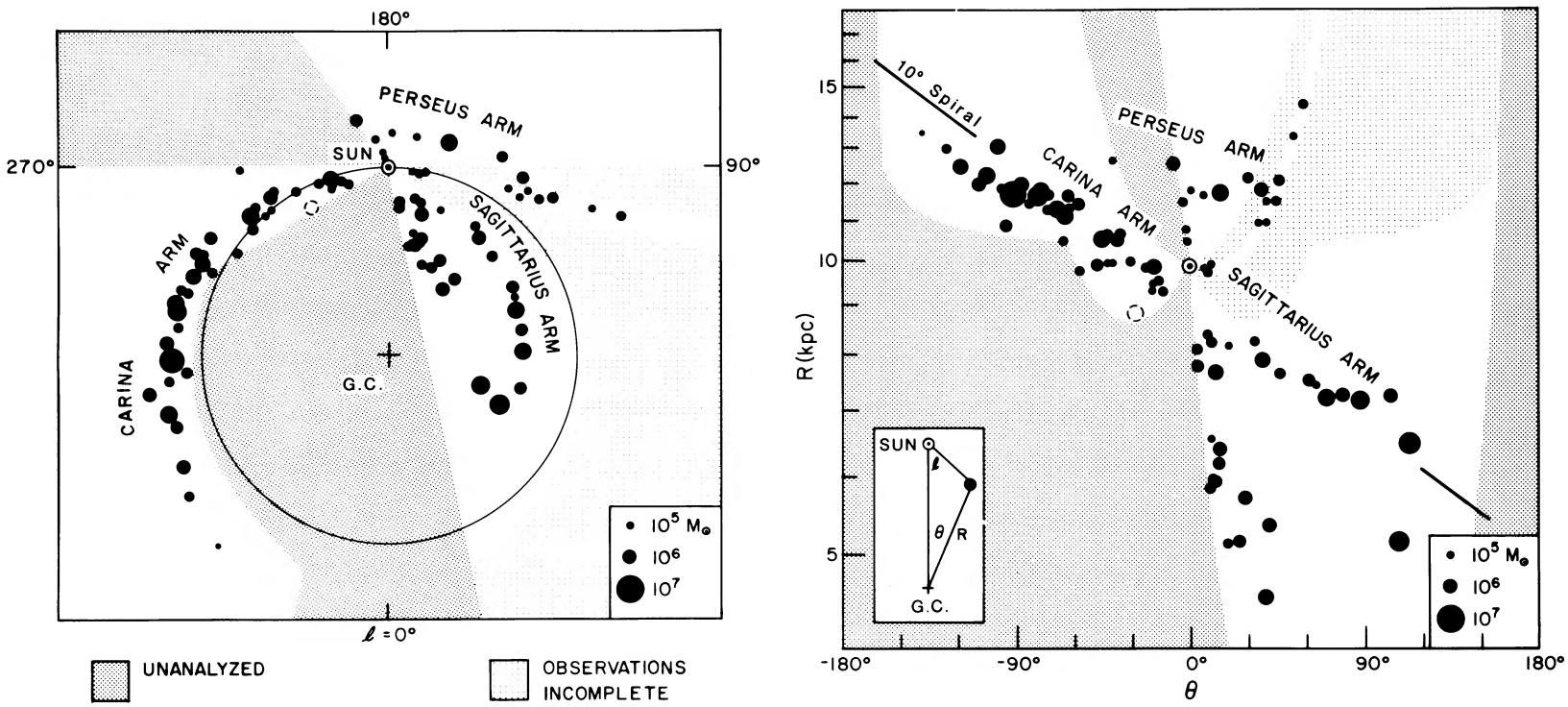

FIG. 3.—(*left*) Face-on view of the Galaxy with locations of the largest molecular clouds. Column densities, hence masses, were calculated by multiplying the integrated CO intensities by 2×10^{20} cm^{-2} K^{-1} km^{-1} s (Lebrun *et al.* 1983). Kinematic distances were determined by using the rotation curve of Burton (1971) inside the solar circle (assumed to be 10 kpc from the galactic center) and a flat curve with a velocity of 250 km s^{-1} beyond the solar circle. The cloud shown with a dashed circle has a very inaccurate kinematic distance and may actually lie in the Carina arm. (*right*) Same clouds shown in Fig. 3 (*left*) replotted in rectangular semilog coordinates. The line follows a 10° logarithmic spiral.

reasonable interpretation of the data is that the Carina and Sagittarius arms form a single 10° spiral arm at least 39 kpc long which extends at least 250° in galactocentric azimuth.

In summary, we find that the tangent point of the Carina arm is exceptionally well outlined by giant molecular clouds; that these clouds trace the Carina arm over more than 20 kpc, longer than for the longest northern features, the Sagittarius and Perseus arms; and that the Carina and Sagittarius features may form a single arm which extends more than two-thirds of the way around the Galaxy.

REFERENCES

Bigay, J. H., Garnier, R., Georgelin, Y. P., and Georgelin, Y. M. 1972, *Astr. Ap.*, **18**, 301.
Burton, W. B. 1971, *Astr. Ap.*, **10**, 76.
Cohen, R. S. 1982, in *Surveys of the Southern Galaxy*, ed. W. B. Burton and F. P. Israel (Dordrecht: Reidel), p. 265.
Cohen, R. S., Cong, H., Dame, T. M., and Thaddeus, P. 1980, *Ap. J. (Letters)*, **239**, L53.
Dame, T. M., Elmegreen, B. G., Cohen, R. S., and Thaddeus, P. 1984, in preparation.
Georgelin, Y. M., and Georgelin, Y. P. 1976, *Astr. Ap.*, **49**, 57.
Graham, J. A. 1970, *A.J.*, **75**, 703.
Gum, C. S. 1955, *Mem. R.A.S.*, **67**, 155.
Hoffleit, D. 1953, *Harvard Ann.*, **119**, 37.
Israel, F. P., *et al.* 1984, *Astr. Ap.*, **134**, 396.
Kerr, F. J. 1983, in *Kinematics, Dynamics, and Structure of the Milky Way*, ed. W. L. H. Shuter (Dordrecht: Reidel), p. 91.
Kerr, F. J., and Kerr, M. 1970, *Ap. Letters*, **6**, 175.
Lebrun, F., *et al.* 1983, *Ap. J.*, **274**, 231.
Mathewson, D. S., Healey, J. R., and Rome, J. M. 1962, *Australian J. Phys.*, **15**, 354.
Rodgers, A. W., Campbell, C. T., and Whiteoak, J. B. 1960, *M.N.R.A.S.*, **121**, 103.
Wilson, T. L., Mezger, P. G., Gardner, F. F. and Milne, D. K. 1970, *Astr. Ap.*, **6**, 364.

L. BRONFMAN, R. S. COHEN, D. A. GRABELSKY, and P. THADDEUS: Goddard Institute for Space Studies, 2880 Broadway, New York, NY 10025

H. ALVAREZ and J. MAY: Departamento de Astronomía, Universidad de Chile, Casilla 36D, Santiago, Chile